Journal of Infrared, Millimeter, and Terahertz Waves
https://doi.org/10.1007/s10762-019-00647-4

Scattering of Terahertz Waves by Snow

Yasith Amarasinghe[1] · Wei Zhang[1] · Rui Zhang[2] · Daniel M. Mittleman[1] · Jianjun Ma[2]

Received: 12 September 2019 / Accepted: 11 November 2019/Published online: 03 December 2019

Abstract
The applications of terahertz (THz) wireless communication require studies on link performance in all kinds of atmospheric conditions, including rain, fog, cloud, haze, and snow. Here, we present theoretical investigations on THz wave propagation in falling snow and through snow layers. Mie scattering theory is employed to fit the measured data. Good agreement confirms the applicability of Mie theory to dry and wet snow when gaseous attenuation and scintillation loss are considered. We investigate the scattering mechanism in a snow layer under different temperatures and water content. We find the THz wave suffers higher signal loss in snow than in rain under identical fall rate.

Keywords Terahertz · Snow · Scattering · Absorption · Scintillation

The technology of terahertz (THz) waves offers wide bandwidth and high capacity for future wireless communications. However, THz waves also suffer from high sensitivity to adverse weather conditions when propagating in the near-surface atmosphere. The path availability and link performance are reduced even in clear weather, as atmosphere gases and air turbulence can lead to link degradation [1–3]. Complete studies on the scattering effect due to weather and gaseous particles are essential for establishing a complete THz channel model. There have been several systematic studies conducted on this under different weather conditions such as rain, fog, haze, cloud, and air turbulence [4–10]. In particular, several investigations of the scattering performance of terahertz waves in snow have been reported [11]. But, there is still a lack of systematic studies because of the difficulties in measurements and characterizations due to the complicated shapes of snow particles. Therefore, a combined approach relying on both theoretical models and case studies is valuable. In this work, we investigate the propagation properties of THz waves in falling snow and a snow layer by considering the effect of snow size distribution, scintillation effect, gaseous attenuation, and temperature variation.

✉ Jianjun Ma
jianjun_ma@bit.edu.cn

[1] School of Engineering, Brown University, Providence, RI 02912, USA

[2] School of Information and Electronics, Beijing Institute of Technology, Beijing 100081, China

1 Physical Characteristics of Snow

As a general statement, a description of the scattering process requires detailed information of numerous snow parameters like shape, dielectric constant, snow size distribution, fall rate, and ambient temperature [12, 13]. These may not all be readily available at a particular site. Snow particles can have a very complicated shape, but generally they do not exhibit any preferred dimension. This poses a significant challenge for snow characterization. Fortunately, earlier research on the scattering by spheroids has demonstrated that the scattering and absorption efficiencies of an ice particle are only weakly dependent on its shape [14]. In addition, photographic measurements have shown that the average ratio of the maximum horizontal dimension to the maximum vertical dimension (i.e., average ellipticity) of falling snow particles is near unity [15]. Hence, a spherical approximation for particle shape is usually assumed for the purpose of simplifying computations and can give a realistic scattering profile [14].

Snow particles are usually regarded as a mixture of ice, air, and water. The dielectric constant of snow can therefore be related to the dielectric constant and volume fraction of each individual component. The dielectric of dry snow, treated as a mixture of ice and air, can be expressed by an empirical formula [16]. Wet snow is a mixture of ice, air, and free water. A two-phase Polder-Van Santen model with ellipsoidal water inclusions is reported for wet snow and shows good agreement with measurements [17]. A modified Debye-like model has a higher accuracy and is more commonly used for frequencies above 15 GHz [18] when dielectric constants of water and ice are available.

The dielectric constant of water can be calculated using a double Debye dielectric model (D3M), which was first developed for seawater based on experimental measurements [19–22]. It can also be reduced to pure water [23] and can be accurately applied in the frequency range up to 1000 GHz [24]. A single Debye model can be used for pure ice (as in [24]), because its relaxation frequency lies in the kilohertz region. The real part of the dielectric constant of ice is essentially independent of frequency up to 1000 GHz and depends only weakly on temperature [25]. As a result, it can be simplified to a constant: $\varepsilon_{ice} = 3.1884$. The imaginary part was calculated in [26], and its validity can be extended to frequencies above 1000 GHz [27, 28].

Another extremely important parameter in calculating scattering phenomena is the snow size distribution. This can be affected by various microphysical and dynamic processes inside and below cloud layers. In practical applications, empirical mathematical formulas derived from the observed size spectra have been used to approximate natural snow size distributions. Unlike raindrops which follow exponential [29, 30], gamma [31], or log-normal distribution [32], snow size distribution is often described by a negative exponential function as shown in Table 1 with a list of all the parameters. In this work, we use snowfall rate (equivalent rainfall rate) instead of visibility, because the latter does not always provide a correct indication of actual snowfall intensity due to the variation in snow type and the differences in the nature of visibility targets during day and night [33].

2 Scattering Attenuation by Falling Snow

The scattering effects of the snow particles on the THz wave are generally analyzed using Mie theory. This is reasonable because the ordinary size of snow particles is in the range from mm to cm [36], which is comparable to or larger than the THz wavelength. This method systematically describes the scattering mechanism of THz waves using particles of various

Table 1 List of negative exponential snow size distributions. (N is the number of snow particle radius of $r + dr$ in unit volume in m^{-3} mm^{-1}; r is the radius of melted snow particles in mm; R is equivalent rainfall rate in mm hr^{-1}; N_0 and Λ are two characteristic parameters and can be retrieved by snowfall rate.)

$N(r) = N_0 \exp(-\Lambda r)$

Source	N_0 (m^{-3} mm^{-1})	Λ (mm^{-1})
Marshall-Palmer [29]	$N_0 = 16 \times 10^3$	$\Lambda = 8.2R^{-0.21}$
Gunn-Marshall [34]	$N_0 = 7.6 \times 10^3 R^{-0.87}$	$\Lambda = 5.1R^{-0.48}$
Sekhon-Srivastava [35]	$N_0 = 5.0 \times 10^3 R^{-0.94}$	$\Lambda = 4.58R^{-0.45}$

sizes in the atmosphere. The scattering characteristics of a THz wave transmitted can be described by the absorption and scattering coefficients. Two important underlying assumptions are required: first, that multiple scattering can be neglected, and second, each scatter behaves independently of all the others. Under those assumptions, the attenuation suffered by a THz wave traveling along a path in snow is [37]

$$\alpha_{\text{snow}} = 4.343 \cdot 10^3 \int_0^\infty \sigma_{\text{ext}}(m,\ r, \lambda)\ N(r) dr, \tag{1}$$

where m is the refractive index of the particle and $N(r)$ is the snow size distribution. σ_{ext} is its extinction cross-section, which is the sum of the absorption cross-section σ_{abs} (m, r, λ) and the scattering cross-section σ_{sca} (m, r, λ): σ_{ext} (m, r, λ) = σ_{abs} (m, r, λ) + σ_{sca} (m, r, λ). The scattering and absorption due to dry and wet snow are calculated and shown in Fig. 1, for a typical equivalent rainfall rate. Here, we use the G-M snow size distribution. We see that the extinction attenuation in dry snow is mainly from the scattering effect because of the low water content. But in wet snow, high water content absorption has comparable influence with the scattering. Below about 800 GHz, the total attenuation is higher in wet snow than in dry snow. However, in this calculation, we do not consider the absorption of the propagating wave by atmospheric gases under different humidity; this effect is important for comparisons with measurements, as shown below.

The total attenuation versus equivalent rainfall rate is shown in Fig. 2 with M-P, G-M, and S-S snow size distributions considered. The measured data and corresponding parameters in [38] are employed in these calculations to verify the validity of our method in the prediction. A discrepancy is observed between the calculations and the measurements in both dry and wet snow, although the G-M prediction matches more closely than the other two. We attribute this

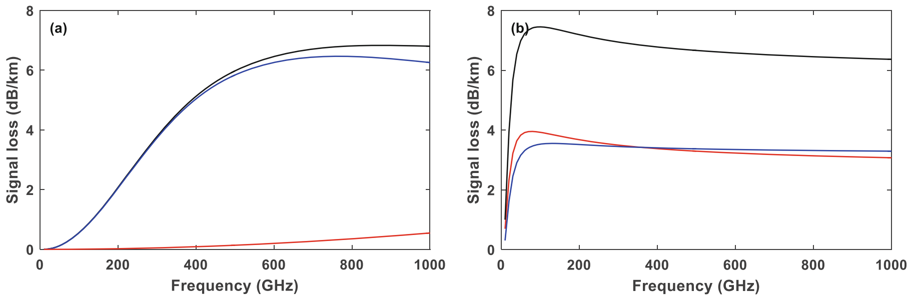

Fig. 1 Signal loss due to (a) dry snow at – 1 °C and (b) wet snow (water content 25%) at 0 °C under the snowfall rate of 10 mm/h. The black curves (total attenuation) are the sum of the red (absorption) and blue (scattering) curves.

discrepancy to the effect of gaseous attenuation (since the humidity ranged from 90 to 97% during these measurements) and to the scintillation effect caused by turbulence. Neither of these effects are accounted for in these calculations.

In clear air, the gaseous composition of atmosphere, mostly water vapor, affects the propagation of THz waves strongly. Water vapor is a minor gaseous constituent but a notably main contributor for the attenuation. The results shown in Fig. 2 suggest the importance of the atmospheric absorption contribution to the total attenuation, even at a frequency of 300 GHz which is far from a water vapor absorption resonance. The gaseous attenuation is commonly described as the sum of spectral absorption links of water vapor and oxygen and a water vapor continuum component. A line-by-line calculation, including also the continuum contribution, is provided by the ITU Recommendation Sector (ITU-R) [39] base on the physical model MPM93 [40]. This method is proved to be valid at frequencies between 1 and 450 GHz, although it is in less good agreement with measurements at higher frequencies [41]. Gaseous spectral attenuation curves corresponding to different relative humidity (RH) are shown in Fig. 3. We see that the operating frequency in Fig. 2 lies in one of the transmission windows, which confirms the maximum propagation distance. Even in the transmission window, the humidity affects the signal attenuation significantly when it changes from 20 to 97%. A 4 dB/km gaseous attenuation can be observed at 300 GHz with a 97% relative humidity. However, it is not simple to account for this effect in our calculation, because the humidity may not be stable during the snowfall. The same influence of humidity in rain was also measured in previous work [42].

In addition to the aforementioned effects, air turbulence and humidity fluctuations can induce a distortion of the wave front of the THz beam, leading to focusing and defocusing effects. Such fluctuations of the beam, called scintillations, would attenuate the beam power and degrade link performance [43, 44]. Falling snow particles are also responsible for the scintillation effect, and the corresponding strength is related to the terminal velocity of snow particles, which was measured as 1.0 to 1.5 m/s for dry snow [36] and 5 or 6 m/s for wet snow [15]. Previously, we have reported the THz link performance in air turbulence introduced by temperature fluctuation, where the scintillation loss can be calculated by

$$\alpha_{\text{scint}} = \left| 10\log\left(1-\sqrt{\sigma^2_{\text{scint}}}\right) \right|, \tag{2}$$

where $\sigma^2{}_{\text{scint}}$ represents the scintillation index and can be used to determine the effect and magnitude of scintillation [45]. It relates to refractive index structure parameter $C^2{}_n$, wavelength λ, and path length L in [46] as

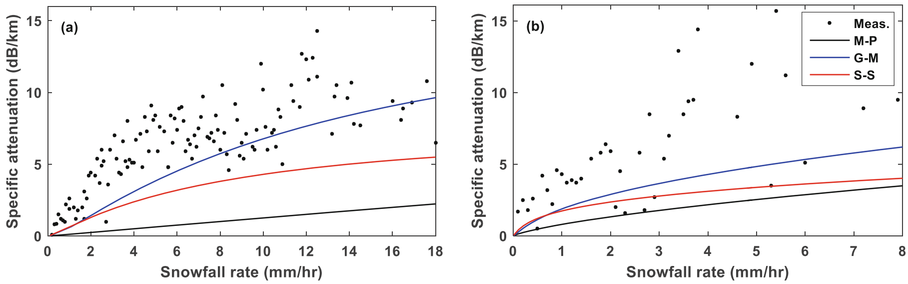

Fig. 2 Measured and calculated signal attenuation at 300 GHz by (a) dry and (b) wet snow.

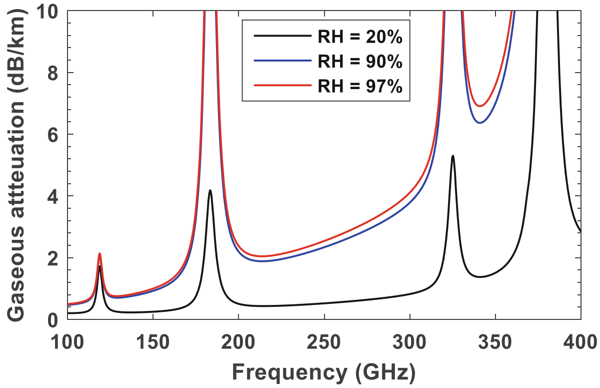

Fig. 3. Attenuation due to atmospheric gases between 100 and 400 GHz. ($T = 0$ °C, $P = 1013$ hPa, and RH = 20%, 90%, and 97%)

$$\sigma_{\text{scint}}^2 = 2 \cdot \sqrt{23.17\left(\frac{2\pi}{\lambda}10^9\right)^{7/6} \cdot C_n^2 \cdot L^{11/6}}. \tag{3}$$

The refractive index structure parameter is a quantitative measure of turbulence and also can be called turbulence strength. Figure 4 shows that the scintillation loss increases exponentially with respect to turbulence strength $C^2{}_n$ and exceeds 0.5 dB/km for strong turbulence ($C^2{}_n >$ 10^{-13}). We conclude that the scintillation loss should also be considered in the calculation, especially over a long propagation distance.

3 Comparison of Attenuation due to Snow and Rain

Due to the high water content in wet snow, the attenuation should be comparable to that due to rain. Dry snow with a much lower water content should lead to an attenuation much less than that due to rain at the same fall rate. But one work reports a 312.5-GHz signal suffers 1–1.5 dB more attenuation due to dry snow than due to rain [47]. Besides, a 7–8 dB more attenuation due to wet snow than due to rain was reported in [48]. They conclude that the attenuation by snow may be more serious for higher frequencies at the THz range. Richard and Federici

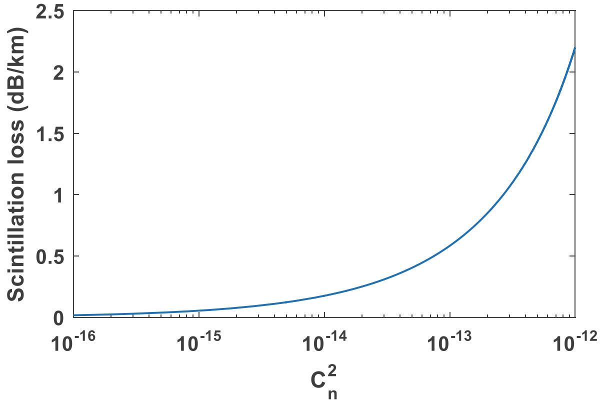

Fig. 4 Scintillation attenuation for THz wave under different turbulence strengths.

attribute the difference to the higher concentration, larger dimension, and irregular shapes of snowflakes with lower fall velocity [49, 50].

To address this question further, we perform a comparison between the effects of snow and rain with the same fall rate (equivalent rainfall rate for dry and wet snow, rainfall rate for rain). In the calculation for rain, the Joss distribution is employed because it shows higher accuracy under light, moderate, and heavy rain conditions compared with Marshall-Palmer (M-P) distribution and Weibull distribution [8]. Mie scattering is also used in the scattering description. The total extinction loss due to rain, dry snow, and wet snow is show in Fig. 5 under the same fall rate. Here, the gaseous attenuation is also included. We can see that the total attenuation at 312.5 GHz due to dry and wet snow is higher than that due to rain, which is consistent with the results in [47]. But this difference becomes smaller for higher frequencies because the absorption due to water vapor becomes much more serious and dominates.

4 Scattering Attenuation by a Snow Layer

In the measurements from [38], the snow cover on antennas would also affect the observed signal loss. So information about the snow layer should be considered. In remote sensing, backscattering behavior from a snow layer is always considered and can be predicted by the radiative transfer model (RTM) with high accuracy [51]. Theoretical predictions have been found to agree well with the experimental measurements with operating frequency at 35, 95, and 140 GHz [52] and 225 GHz [53]. An accurate understanding of the frequency dependence of the propagation loss of THz waves in a snow layer could be used to estimate the thickness of a snow layer covering on antennas.

In the calculation of propagation properties in a snow layer, a different method should be considered. A layer of dry snow can be considered a dielectric medium consisting of ice crystals in an air background. Wet snow layer is somewhat more complicated since the medium becomes a mixture of ice particles, water droplets, and air. The water droplets are usually much smaller than the ice particles and are evaluated by a volumetric water content of snow (also called snow wetness, m_v), which cannot exceed 30%. So the scattering effect in the dry and wet snow is mainly caused by the ice particles. The background medium can be regarded as air or a mixture of water droplets and air. Since the ice particles are comparable in size to the wavelength, we can still use Mie scattering theory to describe this process.

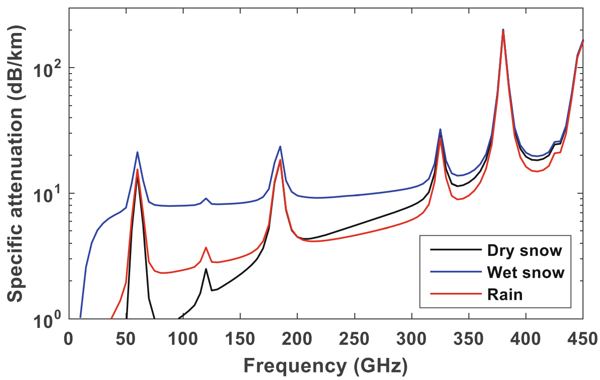

Fig. 5 Signal attenuation due to (a) rain at 20 °C, (b) dry snow at −1 °C, and (c) wet snow (wetness 25%) at 0 °C under a fall rate of 10 mm/h.

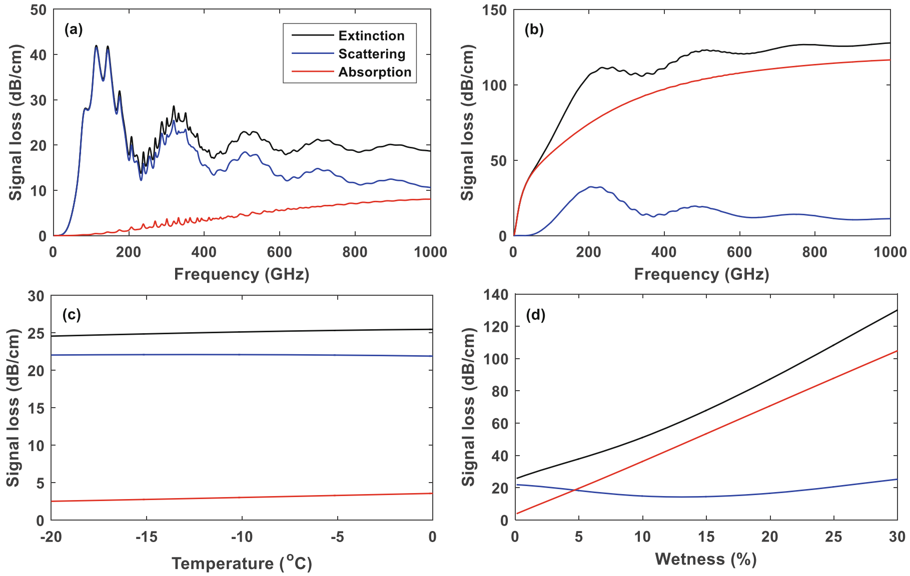

Fig. 6 Attenuation of THz wave in (a) dry cover with temperature at − 1 °C and (b) wet snow covers with a 20% wetness; signal loss with respect to (c) temperature and (d) wetness.

In Fig. 6, we show the calculated signal loss due to scattering, absorption, and their sum (total extinction) when THz waves propagate in dry and wet snow layers with 97% humidity. Figure 6 (a) shows the signal loss spectrum due to a dry snow layer at − 1 °C. The loss oscillates with an increase of the frequency, and the period changes with the variation of average ice particle size. We can see that the loss is mainly due to the scattering in dry snow, while absorption has only a small influence, especially in the lower frequency range. When we change the snow temperature from 0 to − 20 °C, we see little change in any of the loss parameters, as in Fig. 6(c). Since there is almost no water inside dry snow and the dielectric constant of ice particles depends only weakly on temperature, this temperature independence is not surprising. However, for wet snow, the absorption due to the liquid water plays a main role as shown in Fig. 6(b). In Fig. 6(d), the absorption increases significantly for high wetness, while the scattering loss is approximately constant.

5 Conclusions

In this paper, we combine meteorological data and Mie scattering theory to investigate the scattering behavior of THz waves in falling snow and in a snow layer. The theoretical results are in rough qualitative agreement with the experimental data when gaseous attenuation and scintillation effect are not considered. Compared with the attenuation by rain, the THz signal suffers higher loss when it propagates in dry and wet snow for frequencies above 200 GHz. Signal loss in a dry snow layer is mainly attributed to scattering effects because of the low water content, and it does not change when the temperature is reduced from 0 to − 20 °C. The absorption effect becomes more serious when snow wetness increases, but the scattering effect is largely unaffected by water content.

Funding Information We appreciate the support by the Beijing Institute of Technology Research Fund Program for Young Scholars. DMM also acknowledges partial support from the US National Science Foundation and from the Air Force Research Laboratory.

References

1. Y. Yang, M. Mandehgar, and D. R. Grischkowsky, “Understanding THz Pulse Propagation in the Atmosphere,” *IEEE Transactions on Terahertz Science and Technology,* vol. 2, pp. 406-415, 2012.
2. J. Ma, L. Moeller, and J. F. Federici, “Experimental Comparison of Terahertz and Infrared Signaling in Controlled Atmospheric Turbulence,” *Journal of Infrared Millimeter and Terahertz Waves,* vol. 36, pp. 130-143, Feb 2015.
3. J. Ma, R. Shrestha, L. Moeller, and D. M. Mittleman, “Invited Article: Channel performance for indoor and outdoor terahertz wireless links,” *APL Photonics,* vol. 3, p. 12, 2018.
4. Y. Yang, M. Mandehgar, and D. R. Grischkowsky, “Broadband THz Signals Propagate Through Dense Fog, ” *IEEE Photonics Technology Letters,* vol. 27, pp. 383-386, 2015.
5. J. Ma, F. Vorrius, L. Lamb, L. Moeller, and J. F. Federici, “Experimental Comparison of Terahertz and Infrared Signaling in Laboratory-Controlled Rain,” *Journal of Infrared Millimeter and Terahertz Waves,* vol. 36, pp. 856-865, Sep 2015.
6. K. Su, L. Moeller, R. B. Barat, and J. F. Federici, “Experimental comparison of terahertz and infrared data signal attenuation in dust clouds,” *Journal of the Optical Society of America a-Optics Image Science and Vision,* vol. 29, pp. 2360-2366, Nov 2012.
7. K. Su, L. Moeller, R. B. Barat, and J. F. Federici, “Experimental comparison of performance degradation from terahertz and infrared wireless links in fog,” *Journal of the Optical Society of America a-Optics Image Science and Vision,* vol. 29, pp. 179-184, Feb 2012.
8. Q. Jing, D. Liu, and J. Tong, “Study on the Scattering Effect of Terahertz Waves in Near-Surface Atmosphere,” *IEEE Access,* vol. 6, pp. 49007-49018, 2018.
9. G. A. Siles, J. M. Riera, and P. Garcia-del-Pino, “Atmospheric Attenuation in Wireless Communication Systems at Millimeter and THz Frequencies,” *IEEE Antennas and Propagation Magazine,* vol. 57, pp. 48-61, 2015.
10. E.-B. Moon, T.-I. Jeon, and D. R. Grischkowsky, “Long-Path THz-TDS Atmospheric Measurements Between Buildings,” *IEEE Transactions on Terahertz Science and Technology,* vol. 5, pp. 742-750, 2015.
11. J. Ma, J. Adelberg, R. Shrestha, L. Moeller, and D. M. Mittleman, “The Effect of Snow on a Terahertz Wireless Data Link,” *Journal of Infrared Millimeter and Terahertz Waves,* vol. 39, pp. 505-508, 2018.
12. T. Harimaya, H. Kodama, and K. Muramoto, “Regional differences in snowflake size distributions,” *Journal of the Meteorological Society of Japan,* vol. 82, pp. 895-903, 2004.
13. C. P. Woods, M. T. Stoelinga, and J. D. Locatelli, “ Size Spectra of Snow Particles Measured in Wintertime Precipitation in the Pacific Northwest,” *Journal of the Atmospheric Sciences,,* vol. 65, pp. 189-205, 2008.
14. D. Atlas, *Advances in Geophysics*: New York: Elsevier, 1964.
15. C. Magono and T. Nakamura, “Aerodynamic Studies of Falling Snowflakes,” *Journal of the Meteorological Society of Japan,* vol. 43, pp. 139-147, 1965.
16. C. Matzler, *Thermal Microwave Radiation: Aplications for Remote Sensing.* Stevenage, UK: Institution of Engineering and Technology, 2006.
17. D. Polder and J. H. van Santeen, “The effective permeability of mixtures of solids,” *Physica,* vol. 12, pp. 257-271, 1946.
18. M. Hallikainen, F. Ulaby, and M. Abdelrazik, “Dielectric properties of snow in the 3 to 37 GHz range,” *IEEE Transactions on Antennas and Propagation,* vol. 34, pp. 1329-1340, 1986.
19. J. Barthel, K. Bachhuber, R. Buchner, and H. Hetzenauer, “Dielectric spectra of some common solvents in the microwave region. Water and lower alcohols,” *Chemical Physics Letters,* vol. 167, pp. 62-66, 1990.
20. J. T. Kindt and C. A. Schmuttenmaer, “Far-Infrared Dielectric Properties of Polar Liquids Probed by Femtosecond Terahertz Pulse Spectroscopy,” *The Journal of Physical Chemistry,* vol. 100, pp. 10373-10379, 1996.
21. A. P. Stogryn, H. T. Bull, K. Rubayi, and S. Iravanchy, “The microwave permittivity of sea and freshwater,” Sacramento, CA 1996.
22. C. Ronne, L. Thrane, P. O. Astrand, A. Wallqvist, K. V. Mikkelsen, and S. R. Keiding, “Investigation of the temprerature dependence of dielectric relaxation in liquid water by THz reflection spectroscopy and molecular dynamics simulation,” *Journal of Chemical Physics,* vol. 107, pp. 5319-5331, 1997.
23. C. Mätzler, *Thermal Microwave Radiation: Applications for Remote Sensing*. UK: Institution of Engineering & Technology, 2007.

24. F. T. Ulaby, R. K. Moore, and A. K. Fung., *Microwave Remote Sensing: Actice and Passive. Vol. 2, Radar remote sensing and surface scattering and emission theory*: Reading, MA: Addison-Wesley, 1982.
25. C. Matzler and U. Wegmuller, "Dielectric properties of freshwater ice at microwave frequencies," *Journal of Physics D: Applied Physics,* vol. 20, pp. 1623-1630, 1987.
26. G. Hufford, "A model for the complex permittivity of ice at frequencies below 1 THz," *International Journal of Infrared and Millimeter Waves,* vol. 12, pp. 677-682, 1991.
27. O. Mishima, D. D. Klug, and E. Whalley, "The far-infrared spectrum of ice Ih in the range 8–25 cm − 1. Sound waves and difference bands, with application to Saturn's rings.," *Journal of Chemical Physics,* vol. 78, pp. 6399-6404, 1983.
28. J. H. Jiang and D. L. Wu, "Ice and water permittivities for millimeter and sub-millimeter remote sensing applications," *Atmospheric Science Letters,* vol. 5, pp. 146-151, 2004.
29. J. S. Marshall and W. M. Palmer, "The distribution of raindrops with size," *Journal of Meteorology,* vol. 5, pp. 165-166, 1948.
30. G. Zhang, M. Xue, Q. Cao, and D. Dawson, "Diagnosing the Intercept Parameter for Exponential Raindrop Size Distribution Based on Video Disdrometer Observations: Model Development," *Journal of Applied Meteorology and Climatology,* vol. 47, pp. 2983-2992, 2008.
31. D. A. de Wolf, "On the Laws-Parsons distribution of raindrop sizes," *Radio Science,* vol. 36, pp. 639-642, 2001.
32. C. Cerro and B. Codina, "Modeling raindrop size distribution and Z(R) relations in the Western Mediterranean Area," *Journal of Applied Meteorology,* vol. 36, pp. 1470-1479, 1997.
33. R. M. Rasmussena, J. Vivekanandana, J. Colea, B. Myersb, and C. Mastersc, "The Estimation of Snowfall Rate Using Visibility," *Journal of Applied Meteorology,* vol. 38, pp. 1542-1563, 1998.
34. K. L. S. Gunn and J. S. Marshall, "The Distribution with Size of Aggregate Snowflakes," *Journal of the Atmospheric Sciences,,* vol. 15, pp. 452-461, 1958.
35. R. S. Sekhon and R. C. Srivastava, "Snow Size Spectra and Radar Reflectivity," *Journal of the Atmospheric Sciences,,* vol. 27, pp. 299-307, 1970.
36. H. R. Pruppacher and J. D. Klett, *Microphysics of clouds and precipitation*. Dordrecht: Kluwer Academic Publishers, 1997.
37. D. Deirmendjian, *Electromagnetic scattering on spherical polydispersions*. New York: American Elsevier Publishing, 1969.
38. F. Norouzian, E. Marchetti, E. Hoare, M. Gashinova, C. Constantinou, P. Gardner, *et al.*, "Low-THz Wave Snow Attenuation," presented at the International Conference on Radar (RADAR), 2018.
39. *Recommendation ITU-R P.676-11: Attenuation by Atmospheric Gases*. Available: https://www.itu.int/dms_pubrec/itu-r/rec/p/R-REC-P.676-11-201609-I!!PDF-E.pdf
40. H. Liebe, G. Hufford, and M. Cotton, "Propagation modeling of moist air and suspended water/ice particles at frequencies below 1000 GHz," presented at the Proceedings of AGARD, 52nd Specialists Meeting of the Electromagnetic Wave Propagation Panel, 1993.
41. J. F. Ohara and D. R. Grischkowsky, "Comment on the Veracity of the ITU-R Recommendation for Atmospheric Attenuation at Terahertz Frequencies," *IEEE Transactions on Terahertz Science and Technology,* vol. 8, pp. 372-375, 2018.
42. J. Ma, F. Vorrius, L. Lamb, L. Moeller, and J. F. Federici, "Comparison of Experimental and Theoretical Determined Terahertz Attenuation in Controlled Rain," *Journal of Infrared Millimeter and Terahertz Waves,* vol. 36, pp. 1195-1202, Dec 2015.
43. S. S. Muhammad, P. Köhldorfer, and E. Leitgeb, "Channel Modeling for Terrestrial Free Space Optical Links," 2005.
44. S. A. Zabidi, W. A. Khateeb, M. R. Islam, and A. W. Naji, "The Effect of Weather on Free Space Optics Communication (FSO) Under Tropical Weather Conditions and a Proposed Setup for Measurement," 2012.
45. B. E. A. Saleh and M. C. Teich, *Fundamentals of photonics*. New York: John Wiley & Sons, 1991.
46. O. Bouchet, *Wireless Optical Telecommunications*: John Wiley & Sons, 2012.
47. Y. S. Babkin, I. A. Iskhakov, A. V. Sokolov, L. I. Stroganov, and Y. V. Sukhonin, "Attenuation of radiation at a wavelength of 0.96 mm in snow," *Radio Engineering and Electronic Physics,* vol. 15, pp. 2171-2174, 1970.
48. T. Oomori and S. Aoyagi, "A presumptive formula for snowfall attenuation of radio waves," *Trans. Inst. Electron. Commun. Eng. Japan,* vol. 54-B, pp. 451-458, 1971.
49. V. W. Richard, J. E. Kammerer, and R. G. Reitz, "140-GHz Attenuation and Optical Visibility Measurements of Fog, Rain and Snow (No. ARBRL-MR-2800)," 1977.
50. D. L. Renaud and J. F. Federici, "Terahertz Attenuation in Snow and Sleet," *Journal of Infrared, Millimeter, and Terahertz Waves,* vol. 40, pp. 868-877, 2019.
51. Y. Kuga, F. T. Ulaby, T. F. Haddock, and R. D. DeRoo, "Millimeter-wave radar scattering from snow 1. Radiative transfer model," *Radio Science,* vol. 26, pp. 329-341, 1991.

52. F. T. Ulaby, T. F. Haddock, R. T. Austin, and Y. Kuga, “Millimeter-wave radar scattering from snow: 2. Comparison of theory with experimental observations,” *Radio Science,* vol. 26, pp. 343-351, 1991.
53. J. M. Baker, J. B. Mead, and R. E. McIntosh, “Forward scatter polarimetric measurements of terrain at 35 and 225 GHz,” presented at the IGARSS ’98. Sensing and Managing the Environment. 1998 IEEE International Geoscience and Remote Sensing. Symposium Proceedings. (Cat. No.98CH36174), Seattle, WA, USA, 1998.